Multi-temporal Optimization of Virtual Power Plant in Energy-frequency Regulation Market Under Uncertainties

Wenping Qin, Xiaozhou Li, Xing Jing, Zhilong Zhu, Ruipeng Lu, and Xiaoqing Han

***Abstract*—The virtual power plant (VPP) facilitates the coordinated optimization of diverse forms of electrical energy through the aggregation and control of distributed energy resources (DERs), offering as a potential resource for frequency regulation to enhance the power system flexibility. To fully exploit the flexibility of DER and enhance the revenue of VPP, this paper proposes a multi-temporal optimization strategy of VPP in the energy-frequency regulation (EFR) market under the uncertainties of wind power (WP), photovoltaic (PV), and market price. Firstly, all schedulable electric vehicles (EVs) are aggregated into an electric vehicle cluster (EVC), and the schedulable domain evaluation model of EVC is established. A day-ahead energy bidding model based on Stackelberg game is also established for VPP and EVC. Secondly, on this basis, the multi-temporal optimization model of VPP in the EFR market is proposed. To manage risks stemming from the uncertainties of WP, PV, and market price, the concept of conditional value at risk (CVaR) is integrated into the strategy, effectively balancing the bidding benefits and associated risks. Finally, the results based on operational data from a provincial electricity market demonstrate that the proposed strategy enhances comprehensive revenue by providing frequency regulation services and encouraging EV response scheduling.**

***Index Terms*—Virtual power plant (VPP), electric vehicle, distributed energy resource (DER), wind power (WP), photo voltaic (PV), uncertainty, frequency regulation, electricity market, energy market, Stackelberg game, conditional value at risk.**

NOMENCLATURE

$\boldsymbol{\Omega}$	Dispatchable domain of electric vehicle cluster (EVC)
α	Confidence level
β	The maximum percentage of load allowed to be shifted
ε_i	Charging/discharging cost factor
η_s	Auxiliary variable indicating fraction of virtual power plant (VPP) revenue over φ for each scenario
$\eta_{i,c}^{ESS}, \eta_{i,d}^{ESS}$	Charging and discharging efficiencies of the i^{th} energy storage system (ESS)
η_c, η_d	Charging and discharging efficiencies of each electric vehicle (EV)
$\lambda_t^{DA}, \lambda_{t,s}^{DA}$	Power purchase and sale prices of VPP in day-ahead (DA) energy market at time t
$\lambda_t^{cap}, \lambda_t^{mile}$	Frequency regulation capacity and mileage compensation price in DA frequency regulation market at time t
λ_t^1-λ_t^6	Introduced binary variables at time t
$\mu_{i,t}$	Grid connection/disconnection status of each EV
$\mu_{i,t}^{GT}, \mu_{i,t}^{su}, \mu_{i,t}^{sd}$	Binary variables indicating operating, start, and stop states of the i^{th} gas turbine (GT) at time t
μ_t^1-μ_t^7	Introduced dual variables at time t
$\pi_t^{DA,c}, \pi_t^{DA,d}$	EV charging and discharging prices in DA energy market at time t
$\pi_t^{c,\min}, \pi_t^{c,\max}$	The minimum and maximum values of charging price at time t set to be 0.8 and 1.2 by VPP
$\pi_t^{d,\min}, \pi_t^{d,\max}$	The minimum and maximum values of discharging price at time t set to be 0.8 and 1.3 by VPP
π_t^c, π_t^d	Time-of-use charging and discharging prices for EV users at time t
ρ_s	Probability corresponding to scenario s
φ	Value at risk (VaR) of VPP revenue
ω	Frequency regulation deviation penalty factor taken as 1.8
ζ	Risk aversion coefficient indicating degree of risk aversion of VPP that ranges from 0 to 1
a_i, b_i, c_i	Fixed, start, and stop costs of the i^{th} GT
c_t, δ_t^{sh}	Power sale price and subsidy from VPP to load customers
C^{EV}	Charging/discharging cost for EVs
$C_t^{GT,DA}, C_t^{ESS,DA}$	Operating costs of GT and ESS in DA energy

Manuscript received: January 29, 2024; revised: May 24, 2024; accepted: October 8, 2024. Date of CrossCheck: October 8, 2024. Date of online publication: October 22, 2024.

This work was supported in part by the National Natural Science Foundation of China (No. 52477115) and (Shanxi) Regional Innovation and Development Joint Fund Project (No. U21A600003).

W. Qin, X. Li (corresponding author), X. Jing, Z. Zhu, R. Lu, and X. Han are with the Key Laboratory of Power System Operation and Control and the Key Laboratory of Cleaner Intelligent Control on Coal & Electricity, Ministry of Education, Taiyuan University of Technology, Taiyuan 030024, China (e-mail: qinwenping@tyut.edu.cn; 1084017242@qq.com; jingxiang0046@link.tyut.edu.cn; zhuzhilong0362@link.tyut.edu.cn; 1481837568@qq.com; hanxiaoqing@tyut.edu.cn).

DOI: 10.35833/MPCE.2024.000118

	market at time t
C_{VaR}	Conditional value at risk (CVaR) of VPP revenue
$E_{i,t}^{\min}, E_{i,t}^{\max}$	The minimum and maximum dispatchable power of the i^{th} EV at time t
E_i^{ESS}	Battery capacity of the i^{th} ESS
E_i^a, E_i^l	Initial and final charges for the i^{th} EV
$E_i^{\min}, E_i^{\max}$	The minimum and maximum battery capacities of the i^{th} EV
F^{DA}	Total revenue of VPP in DA energy market
f^{up}, f^{dn}	Upward and downward automatic generation control (AGC) frequency regulation commands
k	Electricity sale coefficient ($k=0.9$)
$l_{i,j}$	Operating slope of the j^{th} segment cost of the i^{th} GT
M	A very big number
m	Frequency regulation mileage factor
N	Set of EVs in EVC
n	Number of ESSs
$P_{t,\max}^{chr}, P_{t,\max}^{dis}$	The maximum charging and discharging power of EVC at time t
$P_{i,\max}^{chr}, P_{i,\max}^{dis}$	The maximum charging and discharging power of the i^{th} EV
$P_t^{sh}, L_{t_D}^s$	Power after controllable load transfer and load transferred during demand response period
P_t^{DA}, S_t^{DA}	Declared purchased and sold electrical energeis of VPP in DA energy market at time t
P_t^{chr}, P_t^{dis}	EV charging and discharging power at time t
$P_{i,t}^{ESS,c}, P_{i,t}^{ESS,d}$	Charging and discharging power of the i^{th} ESS at time t
$P_{i,j,t}^{GT}$	The j^{th} segment output of the i^{th} GT at time t
$P_{i,\min}, P_{i,\max}$	The minimum and maximum outputs of the i^{th} GT
$P_{i,\max}^{ESS}$	The maximum charging and discharging power of the i^{th} ESS
$P_{i,t}^{cap}, P_{i,t}^{mile}$	Capacity and mileage of the i^{th} ESS at time t
$P_{i,\max}^{cap}$	The maximum frequency regulation capacity allowed for the i^{th} ESS
$P_t^{w,DA}, P_t^{p,DA}$	Predicted value of wind power (WP) and photovoltaic (PV) in DA energy market at time t
P_t^l	Power of load demand at time t
$P_{i,t}^{FM,c}, P_{i,t}^{FM,d}$	Charging and discharging power of the i^{th} ESS in response to AGC command at time t
$R_t^{EN,DA}, R_t^{FR,DA}$	Revenues of VPP participating in DA energy market and frequency regulation market at time t
R_t^{EV}, R_t^{Load}	Payment costs from EVC and load to VPP at time t
r_t^{cap}	Declared frequency regulation capacity in frequency regulation market at time t
r_i	Climb rate of the i^{th} GT
S_1, S_T	Battery power at initial moment and moment T
$S_{t,\min}^{EV}, S_{t,\max}^{EV}$	The minimum and maximum power of EVC at time t
S, s	Typical set of scenarios and index of scenario
S_t^{DA}	VPP power sales in DA stage
$SOC_{i,t}$	State of charge (SOC) of the i^{th} ESS at time t
$SOC_{i,\min}$, $SOC_{i,\max}$	The minimum and maximum SOC allowed for the i^{th} ESS
T_a, T_l	Grid connection (EV arriving) time and grid disconnection (EV leaving) time
T, T_i	EV dispatchable hour and dispatchable time slot for the i^{th} EV
V	The maximum power of VPP purchased and sold
$z_t^{DA}, z_{i,t}^{ESS}, z_t^{EV}$	Binary variables indicating purchasing and selling status of VPP in DA energy market, and charging/discharging statuses of ESS and EV at time t

I. Introduction

In line with China's goals of carbon peaking and carbon neutrality, the National Energy Administration published the "Blue Book of New Power System Development" in June, 2023 [1]. This significant publication emphasizes that China's new power system is currently in an accelerated transition phase, underscoring the importance of efficient development and utilization of new energy sources to facilitate its construction. However, the direct involvement of distributed energy resources (DERs) in power system operations faces challenges due to their limited individual capacities and extensive geographical dispersion [2], [3]. Furthermore, the regulatory potential of massive DERs needs to be tapped. In response to this challenge, virtual power plants (VPPs) utilize advanced communication technology to aggregate DERs, eliminating spatial and grid constraints. This enhances the regulatory capabilities of the power system and expands collective benefits. Therefore, VPPs have emerged as a pivotal option for the development of new power systems, particularly in dealing with the large-scale integration of DERs [4], [5].

The current focus of research in the field of VPP lies in three main areas: dynamic aggregation [6], [7], power market trading [8], [9], and economic dispatch [10], [11]. In [12], a distributed robust algorithm for VPP peer-to-peer (P2P) energy trading is proposed, considering the imbalance problem and communication failure in the distribution network. The algorithm improves the robustness to communication failures such as network-layer packet loss and computing node failure. Reference [13] comprehensively analyzes the uncertainties arising from renewable energy generation, market price, and load within VPP, and proposes corresponding optimization methods to address these challenges. Reference [14] integrates waste gasification devices into the VPP, and establishes a waste to energy virtual power plant (WtE-VPP) system. This study systematically analyzes the interrelationship between power generation and hydrogen production in WtE-VPP, and proposes a dual-layer clearing model for WtE-VPP participation in combined electricity and hydrogen markets. The model in [14] not only achieves environmentally sound waste utilization and enhances resource efficiency, but also enables the VPP to participate in diverse coupled markets for expanded revenue. Relying on a diversified energy portfolio, flexible energy supply modalities, and abundant energy storage systems, VPP possesses the capability to orchestrate the involvement of distributed generation, controllable loads, and energy storage units in electricity markets. Furthermore, VPPs have the potential to provide supplementary auxiliary services to the power system.

Amidst the ongoing evolution of electricity market reforms, various regions in China have sequentially introduced the policies about VPP participation in the ancillary service market. These regulations are designed to incentivize VPPs to leverage their inherent flexibility, contributing auxiliary services including reserve capacity, peak shaving, and frequency regulation to the power system. A game-theoretic method is employed in [15] to establish a peaking bidding strategy for VPP equipped with controllable DERs and flexible loads. This strategy effectively enhances the enthusiasm of internal VPP members and improves the peaking benefits. Reference [16] proposes an optimal day-ahead (DA) bidding strategy for VPP participating in energy and peak shaving considering the presence of uncertainties. Reference [17] designs a decentralized market clearing strategy to incentivize internal units of VPP to contribute frequency regulation services. This strategy effectively mitigates the reluctance of VPP internal units to adhere to scheduled directives, resulting in a reduction of losses from approximately 80% to around 6%. However, current research predominantly concentrates on individual electricity markets, including energy, peak shaving, and frequency regulation. When engaged in the energy market, VPP prioritizes DA planning, while the involvement in the frequency regulation market emphasizes real-time (RT) efficacy. The decision objectives of VPP are incongruent when participating in these two categories of combined markets, i.e., DA and RT. Therefore, it is of great significance to build a strategy of VPPs participating in the energy-frequency regulation (EFR) market to improve the economy and flexibility of VPP.

To enhance demand-side capacity and strengthen response capabilities, electric vehicles (EVs) have gained attention as unique electric loads with storage and load attributes, thereby emerging as a primary aggregation target for VPP [18]. In [19], a three-stage bidding model is established that incorporates demand response from a single EV for VPP participation in the DA, RT, and equilibrium markets. References [20] and [21] develop a two-stage optimal dispatching model to minimize EV charging costs, while [22] formulates a VPP participation model for frequency modulation of automatic generation control (AGC) that considers EV uncertainties and evaluates the EV compensation tariff based on the EV response deviation threshold. The VPP and EV operators belong to different decision-making entities, and their decision-making objectives exhibit certain conflicts. The purpose of the VPP operator is to maximize the operational benefits of the VPP, whereas that of the EV operator is to reduce the charging cost. Therefore, it has become vital to coordinate the relationship between the rest of VPPs and the EV charging-discharging strategy, and maintain the interests of the two operators for keeping the stable operation of the VPP system.

The bidding behavior of VPP in the DA market can be likened to portfolio behavior [23], which requires consideration of risks arising from uncertainties. Reference [24] uses the information gap decision theory (IGDT) to manage the risks caused by the uncertainties of wind power (WP) and market price. In [25], a risk stochastic optimization method based on conditional value at risk (CVaR) is proposed. Compared with IGDT, this method quantifies the benefits of risk-seeking and makes full use of the statistical characteristics of uncertain parameters to manage expected profits more accurately and flexibly. In [26], CVaR is utilized to establish a two-stage risk aversion model for VPP, leading to the development of optimal bidding strategies for VPP participating in the energy market. In [27], a P2P multi-VPP trading model has been developed that incorporates risk and resolves P2P trades through CVaR risk measurement. However, these studies solely focus on addressing risk concerns in the energy market, necessitating further investigation into the risk management of bidding for participation in the EFR market.

This paper proposes a multi-temporal optimization strategy of VPP in the EFR market under uncertainties, and establishes a Stackelberg game model between VPP and EV to maintain the interests of both parties. The major contributions of this paper are as follows.

1) This paper aggregates all EVs participating in VPP scheduling as an electric vehicle cluster (EVC). An evaluation model of EVC schedulable domain is established, and a Stackelberg game model between VPP and EV is proposed to maintain the interest relationship between them effectively.

2) This paper proposes a multi-temporal optimization strategy for VPP to coordinate internal entities participating in the EFR market. The proposed strategy comprehensively addresses distinct decision objectives of VPP in these two market categories and enhances the overall revenue of VPP.

3) This paper introduces the concept of CVaR in the proposed strategy to manage the risks caused by the uncertainties of WP, photovoltaic (PV), and electricity prices when participating in the EFR market. This provides a reference for VPP operators to develop market strategies based on their risk aversion level.

II. VPP Participating in EFR Market

A. VPP Optimization Strategy

According to the "Virtual Power Plant Construction and Operation Management Code" of a specific province of China [28], this paper presents a comprehensive framework for the consolidation of DERs including WP, PV, gas turbines (GTs), EVs, energy storage system (ESS), and controllable loads, within a "source-grid-load-storage integrated" VPP. The VPP dispatch center actively participates in the EFR market while internally coordinating the operations of its member resources to facilitate market trade. The market coordinated optimization strategy of the VPP is illustrated in Fig. 1.

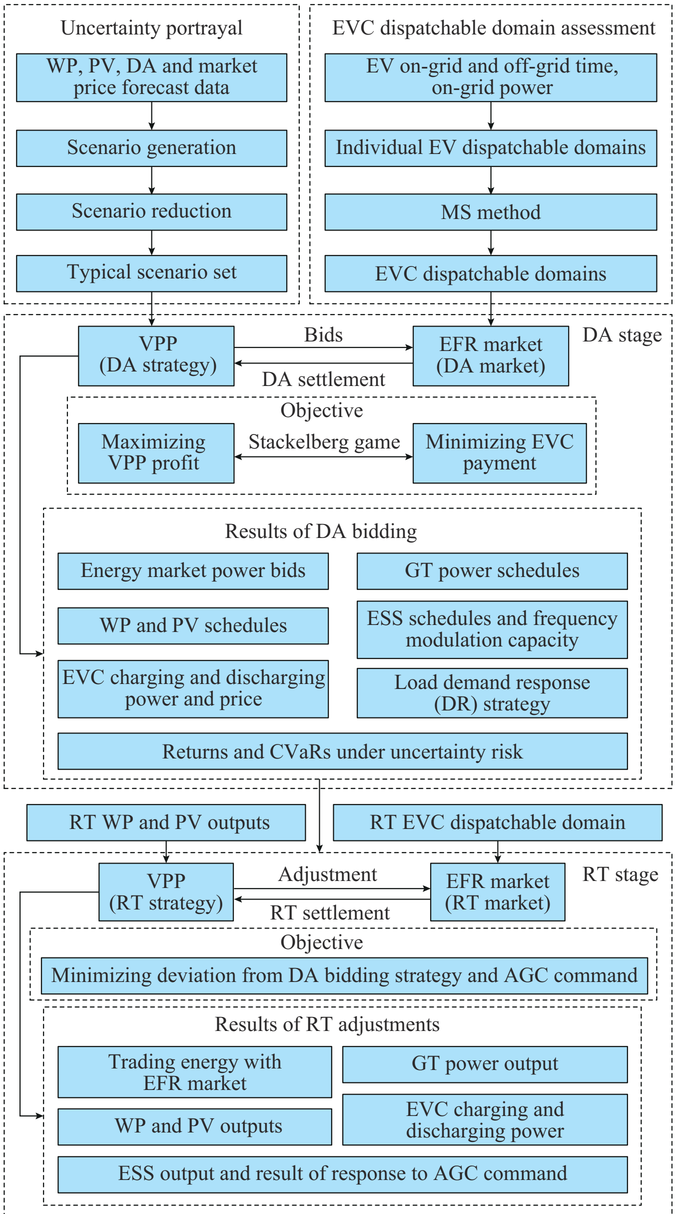

Fig. 1. Market coordination optimization strategy of VPP.

B. Scenarios with Uncertainties of WP, PV, and Market Price

In this subsection, deterministic scenarios are employed to capture the uncertainties of WP, PV, and DA market prices. A multitude of scenarios are generated using a sampling method based on probability density functions derived from forecasting errors. To accurately capture the distribution range of forecasting errors, Latin hypercube sampling (LHS) is employed. It is necessary to generate many scenarios to accurately describe uncertainties, but this significantly increases the computational burden of the model. Therefore, it is necessary to reduce the number of generated scenarios while ensuring a certain level of computational accuracy, to obtain a set of typical scenarios along with their corresponding probabilities. In this paper, the K-means++ algorithm is utilized to reduce scenarios. It allows for updating centroids by traversing the dataset and overcomes the dependency on initial centroids compared with the K-means algorithm [29].

C. EVC Dispatchable Domain Assessment Model

The integration of EVs into the power system exhibits inherent stochastic behavior, and their participation in VPP scheduling is contingent upon the preferences of individual user. To achieve effective scheduling of EVs, all EVs participating in VPP scheduling are aggregated as an EVC in this paper, and an assessment model for the EVC scheduling domain is established.

The dispatchable domain of EV is determined by factors such as its charging and discharging power limitations as well as the available power capacity. Thus, this paper defines the dispatchable domain of EV as encompassing both the dispatchable power domain and its dispatchable energy domain. The model for assessing the dispatchable domain of an individual EV is presented as:

$$\begin{cases} \boldsymbol{\Omega}_i=[P_{i,\max}^{chr}, P_{i,\max}^{dis}, E_{i,t}^{\max}, E_{i,t}^{\min}] \quad t\in[T_a, T_l] \\ E_{i,t}^{\max}=\min\{E_i^a+P_{i,\max}^{chr}(t-T_a)\Delta t\eta^c, E_i^{\max}, E_i^l\} \\ E_{i,t}^{\min}=\max\{E_i^a+P_{i,\max}^{dis}(t-T_a)\Delta t/\eta^d, E_i^{\min}\} \end{cases} \tag{1}$$

Due to variations in the connection time T_i of individual EVs to the power system, their dispatchable period intervals also differ. To ensure consistent dispatchable period intervals, a binary variable $\mu_{i,t}$ is introduced to represent the grid connection and disconnection status of each EV. The scheduling hours of all EVs are extended so that they maintain scheduling consistency. Subsequently, for the sake of simplifying the computational process, the MS method [30] is utilized to map the dispatchable domain of each EV onto a unified domain. In this paper, the decision variables of individual EVs are converted into decision variables of EVCs by the MS method. The model for mapping the EVC dispatchable domain is presented in (2), and the EVC dispatchable domain is established. An intuitive visualization of EVC dispatchable domain mapping process is illustrated in Fig. 2, where the x-axis is the EVC dispatchable time, the y-axis is the EVC power, the z-axis is the individual EV number (EV_i means the i^{th} EV), and the shaded area is the dispatchable domain, of which different colors represent different EVs.

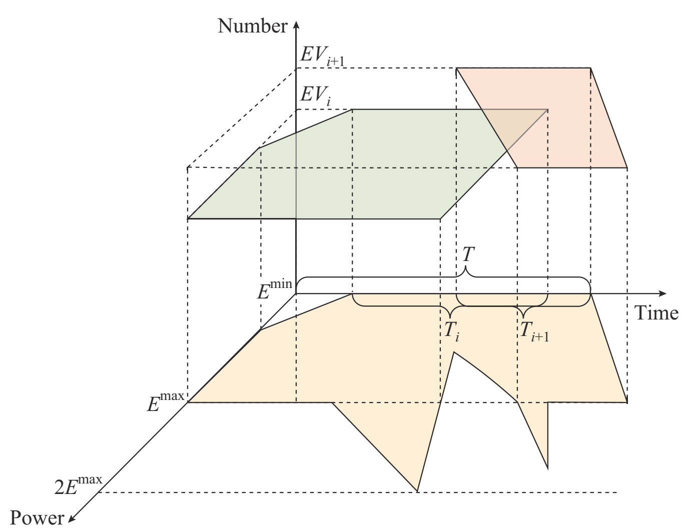

Fig. 2. Illustration of EVC dispatchable domain mapping process.

$$\begin{cases} P_{t,\max}^{chr} = \sum_{i \in N} \mu_{i,t} P_{i,\max}^{chr} \\ P_{t,\max}^{dis} = \sum_{i \in N} \mu_{i,t} P_{i,\max}^{dis} \\ S_{t,\max}^{EV} = \sum_{i \in N} \mu_{i,t} E_{i,t}^{\max} \\ S_{t,\min}^{EV} = \sum_{i \in N} \mu_{i,t} E_{i,t}^{\min} \end{cases} \tag{2}$$

The decision variables of individual EVs are transformed into the decision variables of the EVC using MS method, which simplifies the problem-solving process. Moreover, the instantaneous energy fluctuations within the EVC schedulable domain, induced by the connection and disconnection of an individual EV, can detrimentally influence the accuracy of the EVC dispatchable domain assessment model. To address this issue, this paper introduces the variable ΔS_t^{EV} serving as a representation for the energy step changes during grid connection and off-grid moments of an EV, as shown in (3).

$$\Delta S_t^{EV} = \sum_{i \in N} (\mu_{i,t} - \mu_{i,t-1})(\mu_{i,t} E_i^a + \mu_{i,t-1} E_i^l) \tag{3}$$

According to (2) and (3), the EVC dispatchable domain can be expressed as $\boldsymbol{\Omega} = [P_{t,\max}^{chr}, P_{t,\max}^{dis}, S_{t,\max}^{EV}, S_{t,\min}^{EV}, \Delta S_t^{EV}]$.

In the DA stage, the VPP initially collects historical data from EVs willing to participate in scheduling. This process yields the historical dispatchable domains of individual EVs. Subsequently, the dispatchable domain of EVC is assessed using the evaluation model, resulting in a dataset of historical dispatchable domains of EVC. Finally, predictive algorithms are applied to process the dataset and determine the DA dispatchable domain. In the RT stage, the dispatchable domain of each time is calculated based on the rolling optimization idea by combining the RT data of EVs, enabling the recalculation of the dispatchable domain of EVC based on the latest information available.

III. Strategic Model For VPP Participation in EFR Market

The strategic model of VPP can be categorized into two components: the DA joint bidding model and the RT adjustment model, based on its participation in the EFR market.

A. DA Joint Bidding Model

The DA joint bidding model is formulated as a bi-level optimization framework based on Stackelberg game. The upper level comprises the VPP optimization model, which incorporates CVaR to account for uncertainty and risk considerations. It establishes a multi-objective optimization model that aims to maximize revenue while minimizing risk. By coordinating the operation of internal units, the VPP devises an optimal joint bidding model and determines the charging and discharging prices for the EVC. The lower level consists of the EVC optimization model, which targets minimizing the payment cost while ensuring efficient energy utilization. Based on the VPP charging and discharging prices, this model optimizes the charging and discharging power for each instance to incentivize EV users to participate in scheduling.

1) Upper-layer VPP Optimization Model

1) Objective function

The VPP aims to optimize its revenue by maximizing the difference between benefits and costs:

$$\max F^{DA} = \sum_{t=1}^{T} (R_t^{EN,DA} + R_t^{FR,DA} + R_t^{EV} + R_t^{Load} - C_t^{GT,DA} - C_t^{ESS,DA}) \Delta t \tag{4}$$

$$R_t^{EN,DA} = k \lambda_t^{DA} S_t^{DA} - \lambda_t^{DA} P_t^{DA} \tag{5}$$

$$R_t^{FR,DA} = (\lambda_t^{cap} + m \lambda_t^{mile} k_p^i) r_t^{cap} \tag{6}$$

$$R_t^{EV} = \pi_t^{DA,c} P_t^{chr} - \pi_t^{DA,d} P_t^{dis} \tag{7}$$

$$R_t^{Load} = c_t P_t^{sh} - \delta_t^{sh} L_{t_D}^{sh} \quad \forall t_D \in T_D \tag{8}$$

$$C_t^{GT,DA} = a_i \mu_{i,t}^{GT} + \sum_{j=1}^{n} l_{i,j} P_{i,j,t}^{GT} + b_i \mu_{i,t}^{su} + c_i \mu_{i,t}^{sd} \tag{9}$$

$$C_t^{ESS,DA} = \varepsilon_i (P_{i,t}^{ESS,c} + P_{i,t}^{ESS,d}) \tag{10}$$

Equations (5) and (6) are the revenues for VPP participating in the market; (7) and (8) are the internal revenues to VPP; and (9) and (10) are the operating costs of the VPP.

2) CVaR objective function considering uncertainty risk

To consider the uncertainty risk of WP, PV, and DA market price, this paper uses the CVaR [31] to trade off the risk and revenue of the VPP DA bidding model.

In the upper-layer VPP optimization model, firstly, the maximum revenue achievable through the DA bidding model in each scenario is calculated. Secondly, the maximum expected revenue of the DA bidding model is determined by weighting the sum of scenario probabilities. Lastly, the objective of risk minimization is incorporated by introducing a risk aversion coefficient, transforming the multi-objective problem of the upper-layer model into a single-objective problem. The final objective function can be expressed as:

$$\begin{cases} \max \left\{ (1-\zeta) \sum_{s=1}^{S} \rho_s F_s^{DA} - \zeta C_{VaR} \right\} \\ C_{VaR} = \varphi + \frac{1}{S}(1-\alpha) \sum_{s=1}^{S} \rho_s \eta_s \end{cases} \tag{11}$$

A larger ζ indicates a more conservative VPP and a higher risk aversion.

3) Constraints

To ensure the safe and stable operation of the power system, there exists a transmission power limit between the VPP and the main power:

$$\begin{cases} 0 \le S_t^{DA} \le V z_t^{DA} \\ 0 \le P_t^{DA} \le V(1 - z_t^{DA}) \end{cases} \tag{12}$$

For the GT, the operational constraints are mainly the upper and lower limits of the output power and climb rate.

$$P_{i,\min} \mu_{i,t}^{GT} \le P_{i,j,t}^{GT} \le P_{i,\max} \mu_{i,t}^{GT} \tag{13}$$

$$-r_i \le P_{i,t}^{GT} - P_{i,t-1}^{GT} \le r_i \tag{14}$$

$$\begin{cases}\mu_{i,t}^{GT}-\mu_{i,t-1}^{GT}\le\mu_{i,t}^{su}\\ \mu_{i,t-1}^{GT}-\mu_{i,t}^{GT}\le\mu_{i,t}^{sd}\end{cases}\tag{15}$$

For the energy storage equipment, the operational constraints are mainly the upper and lower limits of the output power and the upper and lower limits of capacity, as shown in (16) and (17).

$$\begin{cases}0\le P_{i,t}^{ESS,c}\le z_{i,t}^{ESS}P_{i,\max}^{ESS}\\ 0\le P_{i,t}^{ESS,d}\le(1-z_{i,t}^{ESS})P_{i,\max}^{ESS}\end{cases}\tag{16}$$

$$SOC_{i,\min}\le SOC_{i,t}\le SOC_{i,\max}\tag{17}$$

$$SOC_{i,t}=\begin{cases}0.5E_i^{ESS}+(P_{i,t}^{ESS,c}\eta_{i,c}^{ESS}-P_{i,t}^{ESS,d}/\eta_{i,d}^{ESS})\Delta t & t=1\\ SOC_{i,t-1}+(P_{i,t}^{ESS,c}\eta_{i,c}^{ESS}-P_{i,t}^{ESS,d}/\eta_{i,d}^{ESS})\Delta t & t\in[2,T]\end{cases}\tag{18}$$

The constraints for frequency regulation capacity declaration mainly involve the remaining capacity constraint after ESS charging and discharging and the frequency regulation mileage constraints.

$$\begin{cases}0\le P_{i,t}^{ESS,c}+P_{i,t}^{cap}\le P_{i,\max}^{ESS}\\ 0\le P_{i,t}^{ESS,d}+P_{i,t}^{cap}\le P_{i,\max}^{ESS}\end{cases}\tag{19}$$

$$\begin{cases}0\le P_{i,t}^{cap}\le P_{i,\max}^{cap}\\ P_{i,\max}^{cap}=0.5E_i^{ESS}\\ \displaystyle\sum_{i=1}^{n}P_{i,t}^{cap}=r_t^{cap}\end{cases}\tag{20}$$

$$0\le P_{i,t}^{mile}\le mP_{i,\max}^{cap}\tag{21}$$

Controllable load constraint needs to ensure that the load demand does not change during the day.

$$-\beta P_t^l\le P_t^l-P_t^{sh}\le\beta P_t^l\tag{22}$$

$$\sum_{t=1}^{T}P_t^l=\sum_{t=1}^{T}P_t^{sh}\tag{23}$$

The power balance constraint is given as:

$$P_t^{DA}+P_t^{dis}+\sum_{i=1}^{n}P_{i,t}^{ESS,d}+\sum_{i=1}^{n}P_{i,t}^{GT}+P_t^{w,DA}+P_t^{p,DA}=S_t^{DA}+P_t^{chr}+P_t^{sh}+\sum_{i=1}^{n_i}P_{i,t}^{ESS,c}\tag{24}$$

To align the charging and discharging price formulated by the VPP with the prevailing market conditions, the VPP establishes pricing based on the time-of-use electricity price of a specific province of China.

$$\begin{cases}\pi_t^{c,\min}\le\pi_t^{DA,c}\le\pi_t^{c,\max}\\ \pi_t^{d,\min}\le\pi_t^{DA,d}\le\pi_t^{d,\max}\\ \dfrac{1}{T}\displaystyle\sum_{t=1}^{T}\pi_t^{DA,c}\le\dfrac{1}{T}\sum_{t=1}^{T}\pi_t^{c}\\ \dfrac{1}{T}\displaystyle\sum_{t=1}^{T}\pi_t^{DA,d}\le\dfrac{1}{T}\sum_{t=1}^{T}\pi_t^{d}\end{cases}\tag{25}$$

2) Lower-level EVC Optimization Model

1) Objective function

The charging and discharging operations of EVC are carried out with the primary goal of minimizing the payment cost. This objective function is expressed as:

$$\min C^{EV}=\sum_{t=1}^{T}(\pi_t^{DA,c}P_t^{chr}-\pi_t^{DA,d}P_t^{dis})\tag{26}$$

2) Constraints

Based on the EVC dispatchable domain assessment model, the former EVC dispatchable domain is calculated and the EVC charging and discharging are constrained, as shown in (27).

$$\begin{cases}0\le P_t^{chr}\le z_t^{EV}P_{t,\max}^{chr}\\ 0\le P_t^{dis}\le(1-z_t^{EV})P_{t,\max}^{dis}\\ S_t^{EV}=S_{t-1}^{EV}+\eta^cP_t^{chr}\Delta t-P_t^{dis}\Delta t/\eta^d+\Delta S_t^{EV}\\ S_{t,\min}^{EV}\le S_t\le S_{t,\max}^{EV}\\ S_T=S_1\end{cases}\tag{27}$$

B. RT Adjustment Model

1) Objective Function

In the RT stage, power output is fine-tuned within a range of ±10% of the deviation from the winning bid of the DA market, taking into account RT data. Meanwhile, the scheduling of ESS is optimized to respond to the AGC command. The objective of this stage is to minimize the deviation of RT output from the result of the winning bid and response to AGC commands, as shown in (28).

$$\min F^{RT}=\sum_{t=1}^{T}\left[\left|S_t^{RT}-S_t^{DA}\right|+\left|P_t^{RT}-P_t^{DA}\right|+\omega(\lambda_t^{cap}+m\lambda_t^{mile}k_p^i)\cdot\left|\sum_{i=1}^{n_i}P_{i,t}^{FM,c}-f^{up}+\sum_{i=1}^{n_i}P_{i,t}^{FM,d}-f^{dn}\right|\right]\Delta t\tag{28}$$

2) Constraints

In response to the AGC command, the ESS should not exceed the declared frequency regulation capacity as:

$$\begin{cases}0\le\displaystyle\sum_{i=1}^{n_i}P_{i,t}^{FM,c}\le f^{up}\\ 0\le\displaystyle\sum_{i=1}^{n_i}P_{i,t}^{FM,d}\le f^{dn}\\ 0\le P_{i,t}^{FM,c}+P_{i,t}^{FM,d}\le P_{i,t}^{cap}\\ 0\le\displaystyle\sum_{i=1}^{n_i}P_{i,t}^{FM,c}+\sum_{i=1}^{n_i}P_{i,t}^{FM,d}\le r_t^{cap}\end{cases}\tag{29}$$

The constraints of ESS remain consistent with (16)-(18), with the addition of upward and downward response power due to frequency regulation signals affecting the charging and discharging power.

The remaining constraints in the RT stage are comparable to those in the DA stage. Please refer to (12)-(15) and (24) for detailed information of these constraints.

IV. Model Transformation and Solution

In the DA joint bidding model, the VPP and EVC are engaged in a Stackelberg game relationship due to conflicting interests. Since both the upper-layer VPP optimization model and lower-layer EVC optimization model are the first-order functions, the Stackelberg game model established in this paper possesses a unique equilibrium solution under the given constraint conditions. However, considering the presence of non-continuous terms in the objective functions of both upper and lower layers, a numerical optimization method based on the Karush-Kuhn-Tucker (KKT) condition [32], [33] is employed. This method effectively transforms the two-layer optimization problem into a mixed-integer linear programming (MILP) problem, allowing for an efficient solution process. The model derivation process is detailed in Supplementary Material A.

Thus, the objective function of the single-level problem can be reformulated as:

$$\begin{cases} \max\left\{(1-\zeta)\sum_{s=1}^{S}\rho_s F_s^{DA}-\zeta C_{VaR}\right\} \\ F_s^{DA}=\sum_{t=1}^{T}[R_t^{EN,DA}+R_t^{FM,DA}+R_t^{Load}-C_t^{GT,DA}- \\ \quad C_t^{ESS,DA}-\mu_t^2 z_t^{EV}P_{t,\max}^{chr}-\mu_t^4(1-z_t^{EV})P_{t,\max}^{dis}+ \\ \quad \mu_t^5 S_{t,\min}^{EV}-\mu_t^6 S_{t,\max}^{EV}+\mu_t^7\Delta S_t^{EV}]\Delta t \end{cases} \tag{30}$$

Equation (30) is subject to constraints (12)-(24) and (S6)-(S12) in Supplementary Material A. Finally, the preceding nonlinear problem is transformed into an MILP problem.

V. Case Study

A. Case Description

To validate the effectiveness of the proposed strategy, a case study is conducted using the electricity market of a specific province of China. The time-of-use electricity price data for the province are presented in Table I. The DA and RT market prices are derived from actual operational data for a selected day in the province, as shown in Fig. 3. The operating parameters for the GT and ESS are presented in Table II and Table III, respectively.

TABLE I
Time-of-use Electricity Price Data

Time	Price (¥/MWh)
Peak period (08:00-11:00, 17:00-23:00)	1004.53
Normal period (07:00-08:00, 13:00-17:00, 23:00-24:00)	676.53
Valley period (00:00-07:00, 11:00-13:00)	375.87

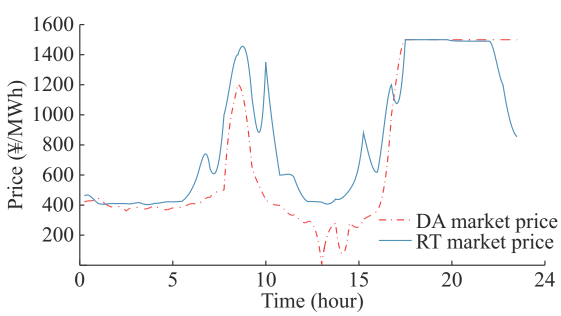

Fig. 3. DA and RT market prices.

TABLE II
Operating Parameters for GT

Number	a_i	b_i	c_i	$P_{i,\max}$	$P_{i,\min}$	r_i
1	500	400	400	5.0	1.5	2.0
2	460	300	300	3.2	1.3	1.5

TABLE III
Operating Parameters for ESS

Number	$P_{i,\max}^{ESS}$	$SOC_{i,\min}$	$SOC_{i,\max}$	$\eta_{i,c}^{ESS}$	$\eta_{i,d}^{ESS}$	λ_i^{cap}	λ_i^{mile}
1	5	0	10	0.95	0.95	10	6
2	7	0	15	0.90	0.90	10	9

In this paper, Monte Carlo simulation is utilized to generate historical and RT EV data. It is assumed that all EVs exhibit uniformity in their battery capacity and maximum charging and discharging power. The EVs have a battery capacity of 32 kWh and a maximum charging and discharging power of 6.6 kW. The SOC ranges from 0.15 to 0.95, with a charging and discharging efficiency of 90%. Two types of EVs are considered in the EVC: nighttime grid-connected EVs and daytime grid-connected EVs. The grid-connection behavior parameters of EVs are presented in Table IV.

TABLE IV
Grid-connected Behavior Parameters of EVs

Type	T_a	T_l	E_i^a	Number
Nighttime	$N(19,2)$	$N(7,2)$	$U(0.3,0.5)$	$U(480,520)$
Daytime	$N(8,1)$	$N(18,1)$	$U(0.2,0.4)$	$U(280,320)$

Note: $N(x,y)$ and $U(x,y)$ denote normal and uniform distributions, respectively.

B. Analysis of Uncertainty Scenarios and EVC Dispatchable Domain

1) Description of Uncertainty Scenarios

To portray the uncertainties of WP, PV, and market price, LHS is used to generate 200 scenarios. These scenarios are then reduced to 5 using the K-means++ algorithm, as shown in Fig. 4. The probabilities of occurrence for each scenario are presented in Table V. The fluctuation of forecast error is assumed to be 10 % of the predicted value.

2) Analysis of EVC Dispatchable Domain

Figure 5 illustrates the EVC dispatchable domains of the EVC during the DA and RT scheduling stages, including the dispatchable power domain and the dispatchable energy domain.

As illustrated in Fig. 5, the EVC dispatchable domain demonstrates a notable consistency across the DA and RT stages, with the most significant deviations observed between hour 17 and hour 19, exhibiting a deviation rate of 9%. The remaining periods exhibit deviations within 5%. The notable variations in the dispatchable domain during this period can be attributed to the increase in the number of EVs connected in the RT stage, which surpasses the DA stage by 33 EVs, thus causing deviations in the dispatchable domains. The dispatchable domain areas gradually expand during the time frame of approximately hours 18-20 as EV users progressively connect their EVs to the grid and accept VPP dispatch, consequently increasing the dispatchable domain areas during this period. During hours 5-8, EVs begin disconnecting from the grid, gradually reducing the areas of EVC dispatchable domain. The observed changes in the EVC dispatchable domain align with users' travelling patterns.

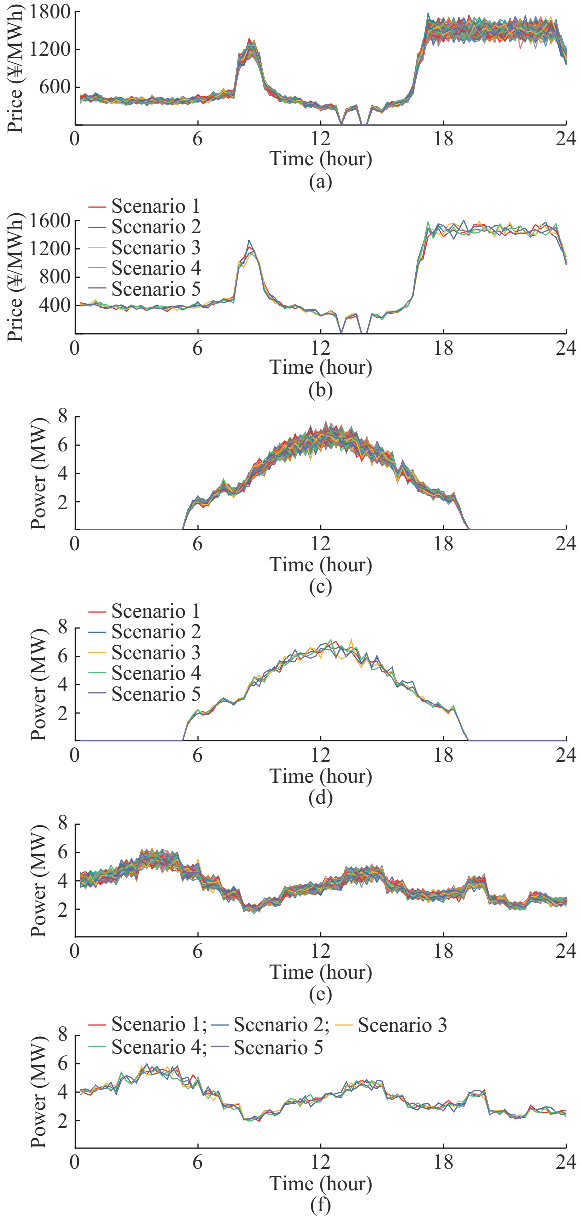

Fig. 4. Generation and reduction of uncertainty scenarios. (a) Market prices for all scenarios. (b) Market prices for five scenarios. (c) PV power for all scenarios. (d) PV power for five scenarios. (e) WP for all scenarios. (f) WP for five scenarios.

TABLE V
PROBABILITIES OF OCCURENCE FOR EACH SCENARIO

Scenario	Probability
1	0.130
2	0.155
3	0.165
4	0.285
5	0.265

C. Analysis of Market Strategy Results of VPP

1) Revenue Analysis with Different Risk Aversion Coefficients

In [24] and [25], the impact of uncertain risks of WP, PV, and market prices on VPP revenue is analyzed, respectively.

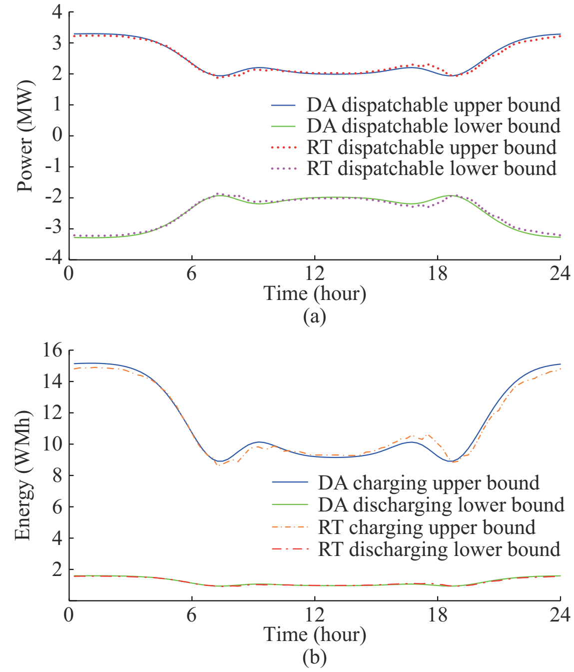

Fig. 5. Dispatchable domains of EVC. (a) Dispatchable power domain. (b) Dispatchable energy domain.

Therefore, on this basis, this paper comprehensively considers the risks caused by the three uncertainties, and uses CVaR to comprehensively analyze the impact of uncertainty risks on VPP revenue based on uncertainty scenarios.

The outcomes of the analysis regarding the DA expected revenues of VPP considering various risk aversion coefficients ζ and their corresponding CVaR are presented in Table VI.

TABLE VI
DA EXPECTED REVENUES OF VPP CONSIDERING VARIOUS RISK AVERSION FACTORS ζ AND THEIR CORRESPONDING CVAR

ζ	DA expected revenue (¥)	CVaR (¥)
0.0	152051	151986
0.2	152039	151659
0.4	151895	151467
0.6	151652	151258
0.8	150987	150785
1.0	150224	149976

As can be seen from Table VI, as the risk aversion coefficient ζ gradually increases, the attitude of VPP towards risk changes from aggressive to conservative, and the expected revenue of the DA bidding gradually decreases. The calculation outcomes presented in Table VI are used to construct the effective frontier curve, illustrating the trade-off between the expected revenue of DA bids and their corresponding CVaR within the DA bidding strategy of VPP, as shown in Fig. 6.

This paper categorizes the risk attitude of VPP into five classifications: aggressive, more aggressive, neutral, more conservative, and conservative, based on their varying degrees of risk aversion. As depicted in Fig. 6, VPPs with an aggressive risk attitude demonstrate relatively stable expected revenue despite increasing the risk-taking levels. Conversely, VPPs with a conservative risk attitude exhibit a smaller increase in expected revenue as risk-taking escalates. For VPPs with a more conservative risk attitude, the relationship between expected revenue and risk-taking levels is linear, where higher risk-taking levels correspond to larger expected returns.

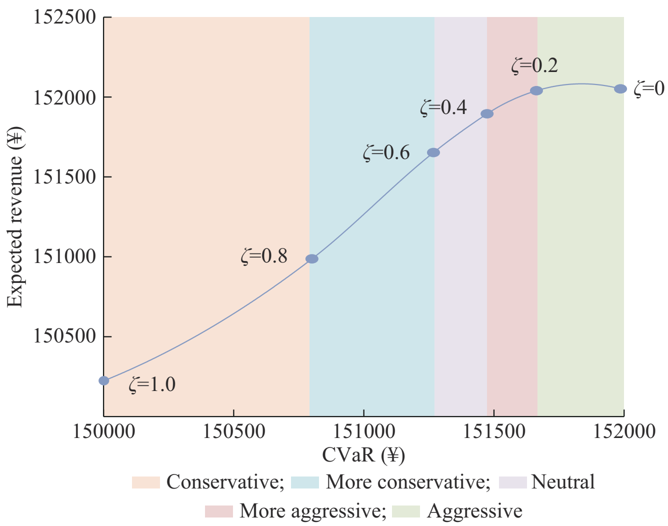

Fig. 6. Efficient frontier curve of expected revenue concerning CVaR.

2) Analysis of Effectiveness of VPP Optimization Strategy

To validate the economic viability of the proposed strategy, three comparative cases are established, considering the uncertainty risk ($\zeta = 0.6$) discussed above.

1) Case 1: the VPP solely participates in the energy market, with EVC undertaking orderly charging and discharging. The charging price follows the time-of-use price shown in Table I, while the discharging tariff is set to be 1.2 times the charging price.

2) Case 2: the VPP solely participates in the energy market, with EVC undertaking orderly charging and discharging. In this case, both the charging and discharging prices are set by the VPP through the Stackelberg game.

3) Case 3: the VPP participates in the EFR market, while EVC continues orderly charging and discharging. The charging and discharging prices are set by the VPP through the Stackelberg game, which aligns with the proposed strategy.

To demonstrate the influence of distinct risk attitudes on VPP dispatch strategies, an additional three sets of comparative experiments are introduced. The cases are described as follows.

1) Case 4: the risk aversion coefficient ζ is 0.2, and the other conditions are the same as Case 3.

2) Case 5: the risk aversion coefficient ζ is 0.4, and the other conditions are the same as Case 3.

3) Case 6: the risk aversion coefficient ζ is 0.8, and the other conditions are the same as Case 3.

Upon conducting the optimization solution calculation, the comparison of revenues in each case is shown in Table VII.

TABLE VII
COMPARISON OF REVENUES IN EACH CASE

Case	DA market (¥)						RT market (¥)		Total revenue (¥)
	Energy market revenue	Frequency regulation market revenue	VPP operating cost	VPP internal revenue	Total market revenue	EVC payment cost	Energy market revenue	Frequency regulation market revenue	
1	55163	0	33950	119700	140913	8817	4962	0	145375
2	57134	0	34399	116840	139575	5957	6219	0	145794
3	55874	13559	34589	116808	151652	5923	5155	–937	156622
4	56274	13376	34393	116794	152051	5912	5065	–923	156193
5	55988	13328	34316	116895	151895	5923	5031	–945	155981
6	54936	13464	34367	116954	150987	5933	5134	–934	155187

As illustrated in Table VII, the initial three cases demonstrate a notable decline in revenue for Case 2, amounting to ¥838 in comparison to Case 1. This is predominantly attributed to the reduction in payment costs associated with EVC, which has been achieved through the implementation of Stackelberg game pricing. This reduction in payment costs indicates a heightened willingness among EV users to actively participate in VPP scheduling, thereby confirming the effectiveness of the Stackelberg game model. Case 2 showcases a higher total revenue in the energy market, which is largely attributable to an increase in the involvement of EVs in scheduling. This enhanced participation contributes to the improved flexibility of the VPP, ultimately resulting in greater revenue generation.

Compared with Case 2, the revenue in Case 3 increases by 7.4%. This notable improvement primarily stems from the simultaneous participation of VPP in both the energy and frequency regulation markets. Despite yielding relatively lower revenue in the energy market, the VPP achieves greater benefits in the frequency regulation market. The distinguishing factor between Cases 2 and 3 lies in the dispatching of ESS for frequency regulation response. This distinction underscores the capacity of VPP to attain higher revenue while incurring lower costs in the frequency regulation market.

By contrasting Cases 3-6, the process of transitioning from a risk aversion coefficient of 0.8 to 0.2 represents a shift from a conservative to an aggressive risk attitude, and the revenue of VPP in the energy market gradually increases. This suggests that aggressive VPP operators are more inclined to participate in market transactions. The income of the frequency regulation market changes little, indicating that the uncertainty risk has a smaller impact on the frequency regulation market. In the RT market, Cases 4 and 5 exhibit lower returns, attributable to significant deviations between the RT and DA outputs of WP and PV, resulting in substantial market deviation costs. In the analysis of the ultimate revenue outcomes, it is evident that aggressive VPP operators stand to gain higher returns, but are also exposed to uncertainty risks, leading to increased deviation costs and a subsequent reduction in the overall revenue.

3) Analysis of Optimization Results of VPP

1) VPP participation in DA EFR market

The optimization of ESS output in the joint bidding decision process is illustrated in Fig. 7. The charging and discharging prices developed by VPP and the scheduling strategy of EVC are shown in Fig. 8.

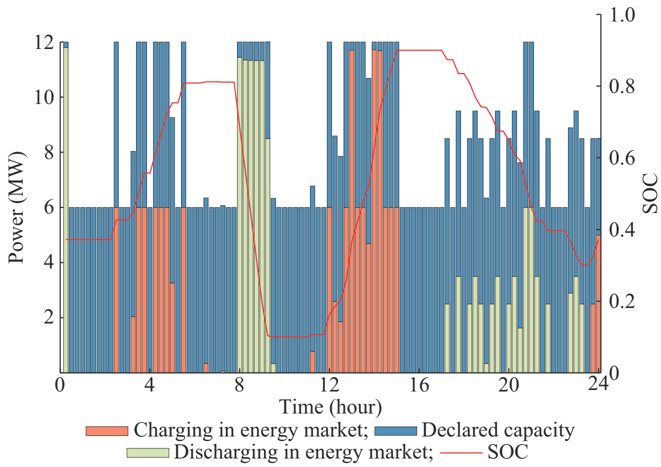

Fig. 7. Optimization of ESS output in joint bidding decision process.

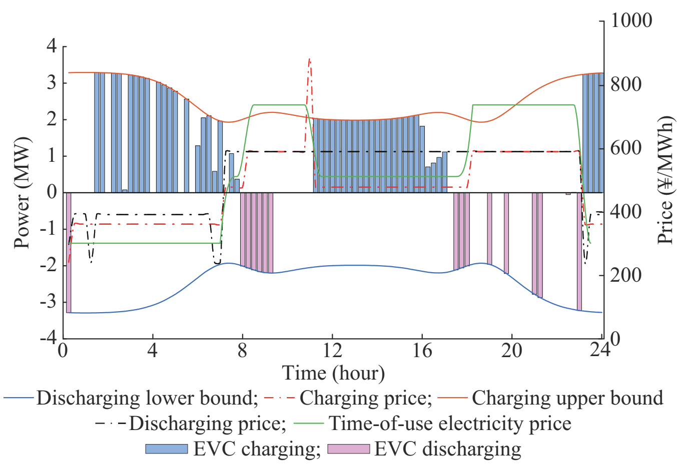

Fig. 8. Charging and discharging prices and scheduling strategy of EVC.

Figure 7 illustrates that the utilization of ESS in the energy market is constrained. The majority of charging occurs between hours 3 and 5 in the morning and between hours 11 and 14 in the afternoon. Conversely, discharging is concentrated between hours 8 and 10 in the morning, and between hours 17 and 22 in the evening. Furthermore, only a single charging or discharging activity takes place during these time slots. Engaging in the frequency regulation market offers benefits beyond revenue generation; it enhances ESS utilization, leveraging its rapid charging and discharging capabilities, and improving dispatch flexibility.

According to Fig. 8, the pricing structure in place for EV charging and discharging incentivizes users to discharge when needed, resulting in higher discharging prices compared with charging prices. EV users, considering their charging requirements, opt to charge during low-price periods and discharge during high-price periods. The pricing set by the VPP fluctuates within a range determined by the time-of-use electricity price, but with smaller variations. This is primarily attributed to the strategic game played between the VPP and EV users, as they seek to maximize their respective interests.

Reference [34] proposes a data-driven two-stage distributed robust optimization model for VPP considering the responsiveness of EVs and the stepped carbon trading mechanism, and employs column and constraint generation (C&CG) to solve the model. Comparing the optimization strategy in [34] with the proposed strategy in this paper, the results in Fig. 9 are obtained.

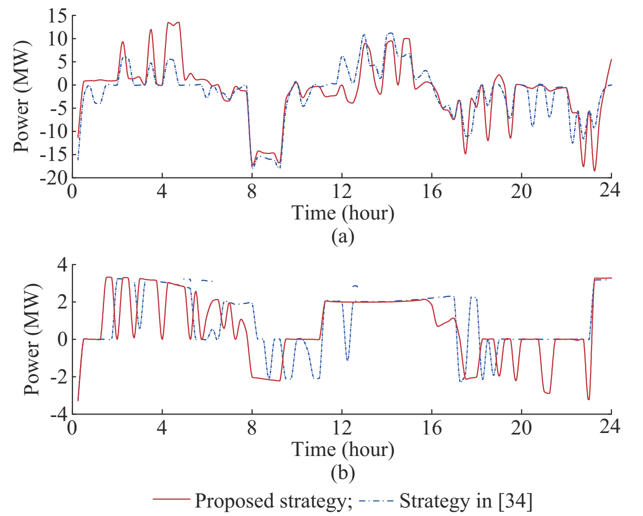

Fig. 9. Comparison of different strategies in DA market of VPP. (a) Power purchased and sold in DA market. (b) EV charging and discharging power in DA market.

As shown in Fig. 9(a), a distributed robust optimization strategy is adopted in [34] to optimize VPPs in the worst scenarios of WP, PV, and market price. Therefore, the strategy in [34] is conservative and will try to dispatch internal unit output as much as possible. Compared with the proposed strategy, the participation in the DA market is not high, and the total market revenue decreases by ¥16972 on the previous day [34]. As shown in Fig. 9(b), [34] considers EV responsiveness for scheduling. Although it improves the enthusiasm for EV response scheduling, compared with the proposed strategy, [34] does not consider EV benefits. There is still room for improvement in the enthusiasm for EV response scheduling. In summary, the proposed strategy has achieved good results compared with that in [34].

2) VPP participation in RT EFR market

Figure 10 presents the analysis results of power purchased and sold in the RT energy market. Figure 11 presents the results of VPP's RT response to AGC commands. Figure 12 presents a detailed comparison of the charging/discharging strategy for EVC in the DA and RT stages. As can be observed from Fig. 10, the results of RT market deviate from the winning bid results of DA market due to uncertainties, resulting in a reduction in the amount of electricity sold and a decrease in revenue. However, the availability of internal generation reduces the cost of purchasing electricity from the electricity market.

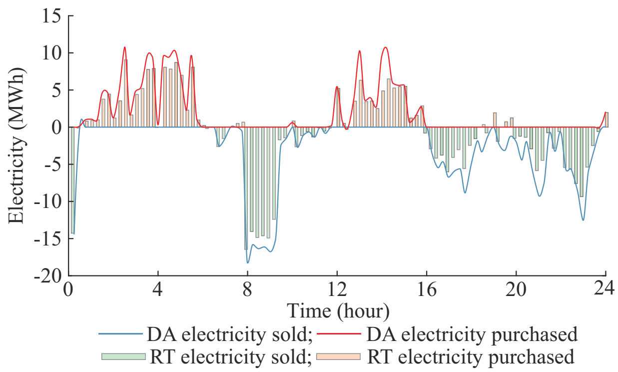

Fig. 10. Analysis results of electricity purchased and sold in RT energy market.

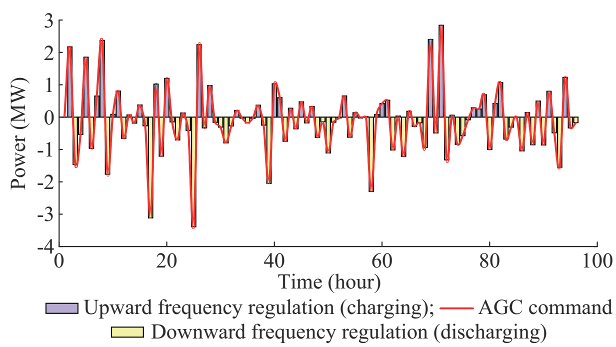

Fig. 11. Results of VPP's RT response to AGC commands.

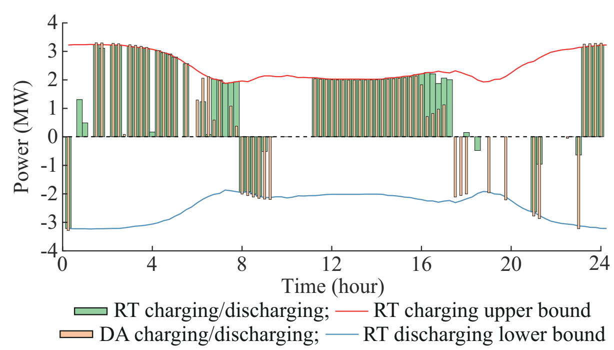

Fig. 12. Detailed comparison of DA and RT charging/discharging for EVC.

As can be observed in Fig. 11, the ESS effectively provides frequency regulation services by employing rapid charging and discharging techniques. It demonstrates the ability to promptly respond to AGC commands with a maximum deviation of 0.45 WM. The VPP showcases successful frequency regulation capabilities through the utilization of ESS, where the internal members collaborate synergistically to fulfill the power requirements of the ESS. This collaborative method markedly diminishes the necessity for external power acquisitions, thereby enhancing the flexibility, cost-effectiveness, and overall efficiency of the ESS in comparison to individual frequency regulation performed solely by the ESS.

As shown in Fig. 12, there is a minimal deviation between the DA and RT stages of EVC charging/discharging, indicating that EVC can effectively track the charging and discharging strategy during the DA stage after adjustments are made during the RT stage. However, during hours 17-22, there is a larger deviation between DA and RT discharging power. This can be attributed to two factors. Firstly, the RT dispatchable domain is lower than the predicted DA dispatchable domain within this period. Secondly, the VPP possesses ample internal discharging resources while the demand for EV discharging is relatively low. The smaller difference between the DA and RT dispatchable domains of EVs enables them to closely adhere to the DA dispatching plan during the RT stage without requiring the re-prediction of EV behavior. This reduction in EV randomness significantly enhances the stability of VPP operations.

VI. Conclusion

This paper proposes a multi-temporal optimization strategy for VPP participating in the EFR market, considering the uncertainties of WP, PV, and market prices. Through simulation analysis, the following conclusions have been drawn.

1) The established EVC dispatchable domain assessment model exhibits a deviation rate of merely 5% when assessing the disparities between DA and RT dispatchable domains for EVC. This reduction in deviations between DA and RT dispatchable domains is advantageous for enhancing the centralized management of EVs by VPP.

2) The Stackelberg game model established between VPP and EVC results in a 32% reduction in user costs for EVC. This demonstrates a positive impact on incentivizing the active participation of EV users in scheduling activities, effectively addressing the issue of balancing interests between VPPs and EVs. Notably, the charging and discharging prices set by VPP for EV dispatching serve as a reference for incentivizing EV users' participation in scheduling.

3) The incorporation of the CVaR theory allows for a balanced consideration of the risk-revenue relationship associated with uncertainties in WP, PV, and market price. This method guides VPP operators in formulating a bidding strategy based on their risk aversion levels.

4) The proposed strategy enables the coordinated operation of EVs and other members for electricity market trades. It effectively harnesses the flexible potential of DERs and achieves the synergy of various forms of DERs.

5) The simulation results indicate that the VPP effectively dispatches the ESS in collaboration with other members to fulfill the frequency regulation response and provide frequency regulation services to the power system. The collaborative behavior has increased VPP revenue by 7.4%, while giving full play to the fast charging and discharging capabilities of ESS.

References

[1] National Energy Administration. (2023, Jun.). Blue Book of New Power System Development of China. [Online]. Available: http://www.nea.gov.cn/2023-06/02/c1310724249.htm

[2] A. Fusco, D. Gioffre, A. Castelli *et al.*, "A multi-stage stochastic programming model for the unit commitment of conventional and virtual power plants bidding in the day-ahead and ancillary services markets,"

Applied Energy, vol. 336, no. 15, p. 120739, Apr. 2023.

[3] L. Peng, F. Zhang, X. Ma *et al.*, "Operation cost optimization method of regional integrated energy system in electricity market environment considering uncertainty," *Journal of Modern Power Systems and Clean Energy*, vol. 11, no. 1, pp. 368-380, Jan. 2023,

[4] H. Gao, T. Jin, G. Wang *et al.*, "Low-carbon dispatching for virtual power plant with aggregated distributed energy storage considering spatiotemporal distribution of cleanness value," *Journal of Modern Power Systems and Clean Energy*, vol. 12, no. 2, pp. 346-358, Mar. 2024.

[5] A. Zahra and H. R. Allah, "Aggregate impact analysis of demand response programs, electric vehicles, and combined heat and power units on integrated management of industrial virtual power plant," *Smart Grids and Sustainable Energy*, vol. 8, no. 2, p. 11, May 2023.

[6] J. Naughton, S. Riaz, M. Cantoni *et al.*, "Comprehensive optimization-based techno-economic assessment of hybrid renewable electricity-hydrogen virtual power plants," *Journal of Modern Power Systems and Clean Energy*, vol. 11, no. 2, pp. 553-566, Mar. 2023.

[7] H. Chen, H. Zhang, and Z. Wang, "A review of market and scheduling characteristic parameter aggregation algorithm of different types of virtual power plants," *Proceedings of the CSEE*, vol. 43, no. 1, pp. 15-28, Jan. 2023.

[8] W. Guo, P. Liu, and X. Shu, "Optimal dispatching of electric-thermal interconnected virtual power plant considering market trading mechanism," *Journal of Cleaner Production*, vol. 279, no. 10, p. 123446, Jan. 2021.

[9] W. S. Sakr, R. A. El-Sehiemy, A. M. Azmy *et al.*, "Identifying optimal border of virtual power plants considering uncertainties and demand response," *Alexandria Engineering Journal*, vol. 61, no. 12, pp 9673-9713, Dec. 2022.

[10] X. Liu, "Research on bidding strategy of virtual power plant considering carbon-electricity integrated market mechanism," *International Journal of Electrical Power & Energy Systems*, vol. 137, p. 107891, May 2022.

[11] M. Rahimi, F. J. Ardakani, and A. J. Ardakani, "Optimal stochastic scheduling of electrical and thermal renewable and non-renewable resources in virtual power plant," *International Journal of Electrical Power & Energy Systems*, vol. 127, p. 106658, May 2021.

[12] X. Wei, J. Liu, Y. Xu *et al.*, "Virtual power plants peer-to-peer energy trading in unbalanced distribution networks: a distributed robust approach against communication failures," *IEEE Transactions on Smart Grid*, vol.15, no. 2, pp. 2017-2029, Mar. 2024.

[13] S. Yu, F. Fang, Y. Liu *et al.*, "Uncertainties of virtual power plant: Problems and countermeasures," *Applied Energy*, vol. 239, no. 1, pp. 454-470, Apr. 2019.

[14] D. Jia, Z. Shen, X. Li *et al.*, "Bi-level scheduling model for a novel virtual power plant incorporating waste incineration power plant and electric waste truck considering waste transportation strategy," *Energy Conversion and Management*, vol. 298, p. 117773, Dec. 2023.

[15] H. Sun, X. Fan, S. Hu *et al.*, "Internal and external coordination bidding strategy of virtual power plant participating in day-ahead power market," *Power System Technology*, vol. 46, no. 4, pp. 1248-1262, Apr. 2022.

[16] Y. Zhang, H. Zhao, and B. Li, "Distributionally robust comprehensive declaration strategy of virtual power plant participating in the power market considering flexible ramping product and uncertainties," *Applied Energy*, vol. 343, p.121133 , Aug. 2023.

[17] X. Sun, H. Xie, D. Qiu *et al.*, "Decentralized frequency regulation service provision for virtual power plants: a best response potential game approach," *Applied Energy*, vol. 352, p. 121987, Dec. 2023.

[18] P. Zhan, L. Xie, R. Ma *et al.*, "Multi-player two-stage low carbon 0ptimal operation strategy considering electric vehicle cluster schedulable ability," *Power System Technology*, vol. 46, no. 18, pp. 147-157, Dec. 2022.

[19] Y. Zhou, G. Sun, W. Huang *et al.*, "Strategic bidding model for virtual power plant in different electricity markets considering electric vehicles and demand response," *Power System Technology*, vol. 41, no. 6, pp. 1759-1767, Mar. 2017.

[20] W. Shi, W. Qin, L. Wang *et al.*, "Regional power grid LSTM dispatch strategy considering the difference between electric vehicle demand and time-of-use electricity price," *Proceedings of the CSEE*, vol. 42, no. 10, pp. 3573-3587, May 2022.

[21] J. Yang, W. Qin, W. Shi *et al.*, "Two-stage optimal dispatching of regional power grid based on electric vehicles' participation in peak-shaving pricing strategy," *Transactions of China Electrotechnical Society*, vol. 37, no. 1, pp. 58-71, Jan. 2022.

[22] G. Yuan and W. Su, "Virtual power plants providing AGC FM service considering uncertainty of electric vehicles," *Power System Technology*, vol. 44, no. 7, pp. 2538-2548, Jul. 2020.

[23] W. Wang, X. Wang, C. Jiang *et al.*, "Day ahead bidding strategy for virtual power plants considering sharpe ratio," *Power System Technology*, vol. 47, no. 4, pp. 1512-1523, Apr. 2023.

[24] A. Khazali, N. Rezaei, W. Su *et al.*, "Risk-aware bilevel optimal offering strategy of a joint wind/storage unit based on information gap decision theory," *IEEE Systems Journal*, vol. 15, no. 2, pp. 1939-1949, Jun. 2021.

[25] D. Xiao, H. Chen, C. Wei *et al.*, "Statistical measure for risk-seeking stochastic wind power offering strategies in electricity markets," *Journal of Modern Power Systems and Clean Energy*, vol. 10, no. 5, pp. 1437-1442, Sept. 2022.

[26] M. V. Dahraie, H. R. Kermani, M. S. Khah *et al.*, "Risk-averse optimal energy and reserve scheduling for virtual power plants incorporating demand response programs," *IEEE Transactions on Smart Grid*, vol. 12, no. 2, pp. 1405-1415, Mar. 2021.

[27] S. Shen, H. Han, Y. Zhou *et al.*, "Electricity-carbon-reserve peer-to-peer trading model for multiple virtual power plants based on conditional value-at-risk," *Automation of Electric Power Systems*, vol. 46, no. 18, pp. 147-157, Aug. 2022.

[28] Shanxi Provincial Energy Bureau. (2022, Jun.). Virtual Power Plant Construction and Operation Management Code, China. [Online]. Available: https://nyj. shanxi. gov. cn/zfxxgk/fdzdgknr/snyjwj/gfxwj/202309/t20230920_9434385.shtml

[29] D. Arthur and S. Vassilvitskii, "K-means++: the advantages of careful seeding," in *Proceedings of the Eighteenth Annual ACM-SIAM Symposium on Discrete Algorithms*, New Orleans, USA, Jan. 2007, pp. 1-6.

[30] X. Zhan, J. Yang, S. Han *et al.*, "Two-stage market bidding strategy of charging station considering schedulable potential capacity of electric vehicle," *Automation of Electric Power Systems*, vol. 45, no. 10, pp. 86-96, May 2021.

[31] R.T. Rockafellar and S. Uryasev, "Optimization of conditional value-at-risk," *The Journal of Risk*, vol. 2, no. 3, pp. 21-41, Jan. 2000.

[32] M. Yu and S. H. Hong, "A real-time demand-response algorithm for smart grids: a Stackelberg game approach," *IEEE Transactions on Smart Grid*, vol. 7, no. 2, pp. 879-888, Mar. 2016.

[33] N. Liu, X. Yu, C. Wang *et al.*, "Energy sharing management for microgrids with PV prosumers: a Stackelberg game approach," *IEEE Transactions on Industrial Informatics*, vol. 13, no. 3, pp. 1088-1098, Jun. 2017.

[34] Y. Chen, Y. Niu, C. Qu *et al.*, "Data-driven-based distributionally robust optimization approach for a virtual power plant considering the responsiveness of electric vehicles and Ladder-type carbon trading," *International Journal of Electrical Power & Energy Systems*, vol. 157, p. 109893, Jun. 2024.

Wenping Qin received the M.S. and Ph.D. degrees from Taiyuan University of Technology (TYUT), Taiyuan, China, in 2001 and 2015, respectively. She is currently a Professor with the College of Electrical and Power Engineering, TYUT. Her research interests include power system reliability analysis and sustainable energy generation technology.

Xiaozhou Li received the B.S. and M.S. degrees from Taiyuan University of Technology (TYUT), Taiyuan, China, in 2021 and 2024, respectively. He is currently working in the State Grid Jibei Electric Power Co., Ltd. Zhangjiakou Power Supply Company, Zhangjiakou, China. His research interests include electricity market, virtual power plant, and economic dispatch.

Xing Jing received the M.S. and Ph.D. degrees from Taiyuan University of Technology (TYUT), Taiyuan, China, in 2020 and 2024, respectively. He is currently working in the State Grid Shanxi Electric Power Company Electric Power Research Institute, Taiyuan, China. His research interests include resilience assessment and improvement of power system.

Zhilong Zhu received the B.S. degree from Taiyuan University of Technology (TYUT), Taiyuan, China, in 2020. He is currently pursuing the Ph.D. degree in electrical engineering from TYUT. His research interests include stability analysis and control of power system.

Ruipeng Lu received the B.S. and M.S. degrees from Taiyuan University of Technology (TYUT), Taiyuan, China, in 2016 and 2019, respectively. He is currently pursuing the Ph.D. degree in electrical engineering from TYUT. His research interest includes power system stability.

Xiaoqing Han received the M.S. and Ph.D. degrees from Taiyuan University of Technology (TYUT), Taiyuan, China, in 1990 and 2009, respectively. She is currently a Professor with the College of Electrical and Power Engineering, TYUT. Her research interests include power system operation and control.